Journal of Electroanalytical Chemistry 935 (2023) 117333

Contents lists available at ScienceDirect

Journal of Electroanalytical Chemistry

journal homepage: www.elsevier.com/locate/jelechem

Normal or parallel configuration in spectroelectrochemistry? Bidimensional spectroelectroanalysis in presence of an antioxidant compound

Fabiola Olmo-Alonso, Jesus Garoz-Ruiz, Aranzazu Heras *, Alvaro Colina *

Department of Chemistry, Universidad de Burgos, Plaza Misael Bañuelos s/n, E-09001 Burgos, SPAIN

ARTICLE INFO

Keywords:
Bidimensional Spectroelectrochemistry
Adrenaline
Ascorbic acid
Quantitative Analysis

ABSTRACT

This work demonstrates how the way a chemical system is sampled plays a key role in spectroelectroanalysis, illustrated by the quantification of an analyte in presence of an antioxidant compound. For this purpose, bidimensional spectroelectrochemistry experiments were performed using epinephrine as the model analyte and ascorbic acid as antioxidant and interfering compound, as a proof of concept. This is the first time that three calibration curves are obtained simultaneously on a single spectroelectrochemistry data set, one for the electrochemical signal and two for the optical responses in normal and parallel configurations. The differences between the two optical arrangements, that are related to the diffusion process which is an essential feature for the spectroelectrochemical detection of compounds, have been experimentally demonstrated. As can be observed, the spectral signal in parallel configuration allows us to obtain the best analytical results, since in this configuration only the first micrometers of the solution adjacent to the electrode surface are sampled, thus removing the interfering effect of the antioxidant compound. This fact does not occur with either the electrochemical signal or the spectral response in normal configuration. Furthermore, it has been shown that the parallel configuration provides better results than the normal configuration in terms of sensitivity. In summary, epinephrine is successfully detected in a simple and effective way, even in the presence of a direct antioxidant compound such as ascorbic acid at different concentrations levels, which makes spectroelectrochemistry a good choice for quantitative analysis.

1. Introduction

Spectroelectrochemistry (*SEC*) is a technique that provides the electrochemical information and the spectroscopic evolution of an electron-transfer process. In this way, signals of different nature are obtained concurrently from a chemical system undergoing an oxidation–reduction process [1–3]. Normal and parallel configuration are the two main optical arrangements for UV–Vis molecular absorption *SEC* [4–8]. On the one hand, in normal configuration, the light beam follows a perpendicular trajectory to the electrode surface, providing information related to changes that occurs both in the solution and at the electrode surface [6,9–11]. This arrangement is characterized by its easy assembly, but its optical pathway is limited to the thickness of the diffusion layer. On the other hand, in parallel configuration (long optical pathway arrangement), the light beam samples only the solution adjacent to the working electrode in parallel direction with respect to its surface, including only information about the spectral changes that take place in the solution closer to the electrode surface [12,13]. The main advantage of this configuration is the longer optical path length compared to the one of the normal configuration, which is associated with higher sensitivity and lower detection limits for soluble compounds [6,11,14]. The main disadvantage could be the assembly due to the difficulties in the alignment of the light beam coming from the light source and going to the detector. However, this drawback can be easily solved by using optical fibers that can be attached to the electrode surface [4].

In 2001, bidimensional *SEC* (BSEC), the simultaneous combination of normal and parallel arrangements, was developed [5]. BSEC provides simultaneously one electrochemical and two spectroscopic signals [4,5]. A light beam samples the system in perpendicular direction to the working electrode surface, meanwhile, a parallel light beam with respect to the electrode surface passes through the solution. Thus, BSEC can distinguish in a single experiment which processes take place in the solution and which ones on the electrode surface during an electrochemical reaction [4–6,11]. Although the use of UV/Vis absorption *SEC* is proving to be of great utility in quantitative analysis

* Corresponding authors.
E-mail addresses: maheras@ubu.es (A. Heras), acolina@ubu.es (A. Colina).

https://doi.org/10.1016/j.jelechem.2023.117333
Received 30 December 2022; Received in revised form 7 March 2023; Accepted 12 March 2023
Available online 16 March 2023

[10,13,15–19], BSEC has never been used for this purpose so far, although it has been widely used for the study of reaction mechanisms and the characterization of conductive polymers [20,21]. In all these works, BSEC has proven to be a very powerful tool that guarantees that all the information obtained is related to the same electrochemical process.

This great potential of BSEC has been exploited in this work to demonstrate an additional advantage of parallel configuration over the normal one, even over the electrochemical response. This advantage is of great utility in quantification of compounds in presence of interfering and antioxidant species. For this purpose, commercial screen-printed electrodes (SPEs) and a fiber-optic based BSEC cell are used to detect the concentration of epinephrine (EP) in presence of ascorbic acid (AA). EP, also known as adrenaline, is a neurotransmitter that plays a fundamental role in human metabolism, regulating physiological processes and acting as chemical messenger [22–25]. Low levels of EP have been found in patients with Parkinson's disease and can result in different mental and physical problems such as anxiety, depression or migraine headaches. EP has been widely studied with electrochemical techniques [26–28], but scarcely with *SEC*, although EP and its oxidation products have well-differentiated spectra [25,29,30]. For its part, AA is considered an essential vitamin in the human diet that can be found in the brain in presence of EP. It has an antioxidant character and it can be considered as a direct interfering species of EP when detected electrochemically [28,31–35]. This type of interference has been previously avoided combining spectroelectrochemistry with multivariate analysis [13,19]. In this work, we avoid the interference of AA in the determination of EP using simple experiments, without any multivariate analysis, and employing the advantages of electrochemistry of controlling the generation of the oxidized compounds.

To demonstrate experimentally the capabilities of BSEC for the analysis of mixtures with interfering species that have antioxidant properties, the main objective of this work is the quantification of EP in the presence of AA, allowing us to select the best configuration for quantitative purposes thanks to the large amount of information provided by BSEC. So, this BSEC study, which had never been carried out before, allows us to distinguish the different results obtained using each configuration and to select the best arrangement for this kind of systems, all in a single experiment.

2. Materials and methods

2.1. Reagents and materials

L(-)-Epinephrine (EP, 99 %, Acros Organics), ascorbic acid (AA, L (+)-Ascorbic acid, ACS reagent, Acros Organics) and perchloric acid ($HClO_4$, 60 %, Panreac) were used as received without further purification. Commercial SPEs (DRP-110, Metrohm-DropSens), which included a three-electrode configuration printed on the same support, were used to perform all the experiments. Each SPE has a 4 mm diameter disk screen-printed carbon working electrode (WE), a carbon counter electrode (CE) and a silver pseudo-reference electrode (RE). In all experiments, cyclic voltammograms (CVs) corresponding to a first scan, starting at a potential where no electrochemical reaction takes place, are shown. All voltammograms are represented respect to a silver pseudo-reference electrode. For comparison with experiments in literature, a difference of +0.588 V respect to a reversible hydrogen electrode (RHE) is measured using the same supporting electrolyte composition, Figure S1, in Supplementary Material (SM).

All solutions were daily prepared using high-quality water (18.2 MΩ cm resistivity at 25 °C, Milli-Q Direct 8, Millipore). All experiments were performed at room temperature.

2.2. Instrumentation

Two customized SPELEC instruments (Metrohm-DropSens), controlled by DropView SPELEC software (Metrohm-DropSens), were used for the BSEC experiments.

2.3. Experimental setup

A bifurcated optical fiber (QBIF600-UV–VIS, Ocean Optics) was connected to the light source. A scheme of the BSEC cell used to perform the experiments is shown in Fig. 1. As can be observed, a reflection probe which consists of 6 illumination optical fibers and a central collection optical fiber was connected to obtain the optical response in normal configuration (FCR-7UV200-2–2.5X100-ME-SR, Avantes). The reflection probe was placed at 1.8 mm from the working electrode using a clamp. In order to obtain the optical response in parallel arrangement, two bare optical fibers (100 μm in diameter, Ocean Optics) were aligned face to face on the working electrode at a distance of 0.2 mm. One of the optical fibers was connected to the light source and the other one to the spectrometer. To perform the corresponding measurements, a solution drop (100 μL) was placed on the electrode, covering the three-electrode system and the ends of the reflection probe and the bare optical fibers. In all experiments the initial solution was taken as reference spectrum.

3. Results and discussion

3.1. BSEC of EP using cyclic voltammetry

The BSEC behavior of EP in acidic medium is shown in Fig. 2. This figure is related to a solution of $2{\cdot}10^{-3}$ M EP in 0.1 M $HClO_4$. As can be observed, the cyclic voltammogram (CV) between −0.20 V and +0.90 V at 0.01 V s^{-1} shows a quasi-reversible behavior (Fig. 2a) with an oxidation peak at +0.28 V and a cathodic one peaking at +0.15 V. At this acidic pH, the oxidation mechanism corresponds to the oxidation of EP to epinephrinequinone (EPQ) [23–25,36]. This oxidation process in acidic media is related to the transfer of two electrons and two protons, with the generation of EPQ, that is regenerated in the backward scan, being the formal potential of +0.215 V. The optical responses in parallel and normal configuration are plotted in Fig. 2b and 2c, respectively. In the two configurations, an absorption band that evolves along the experiment can be observed centered at 385 nm, corresponding to the oxidation of EP to the appropriate quinone. Fig. 2d displays the cyclic voltabsorptograms (CVAs) at 385 nm for the two optical configurations. In parallel arrangement, a quasi-stationary stage is reached at the end of the forward scan. At this point, the absorbance achieves an almost constant value (around 0.37 a.u.) because the optical fibers only sampled approximately the first 120 μm closest to the working electrode surface (diameter of the optical fibers attached to the electrode surface, 100 μm, covered by a cladding). However, all the diffusion layer is sampled in normal configuration, and the absorbance continues to increase in the cathodic scan until the potential is low enough to reduce the EPQ generated. It should be remarked that, in both CVAs, absorbance starts to increase at the same potential, around +0.20 V due to the oxidation of EP to EPQ. In the same way, absorbance also starts to decrease at the same potential in the backward scan due to the reduction of EPQ to EP, around +0.19 V. As it is explained in the introduction section, the main advantage of BSEC is that it provides in a single experiment one electrochemical and two spectroscopic signals simultaneously, all of them related to a single system, in this case the oxidation of EP. This multirresponse technique avoids problems of data correlation when consecutive experiments are performed, due to the difficulty of achieving exactly the same experimental conditions. Fig. 2 also reveals that the absorbance signal in parallel configuration is remarkably

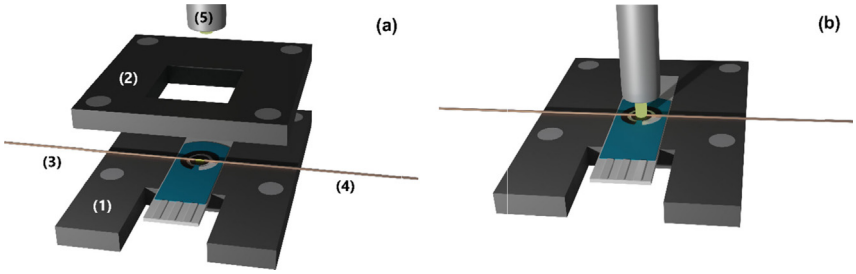

Fig. 1. Schematic view of the BSEC cell (a) disassembled and (b) assembled; upper body has been removed to clearly observe the position of the optical fibers in the assembled cell. (1) Lower body for supporting the screen-printed electrode (2) upper body to fix the electrode (3) illumination optical fiber in parallel configuration (4) collection optical fiber in parallel configuration and (5) reflection probe for normal configuration measurements.

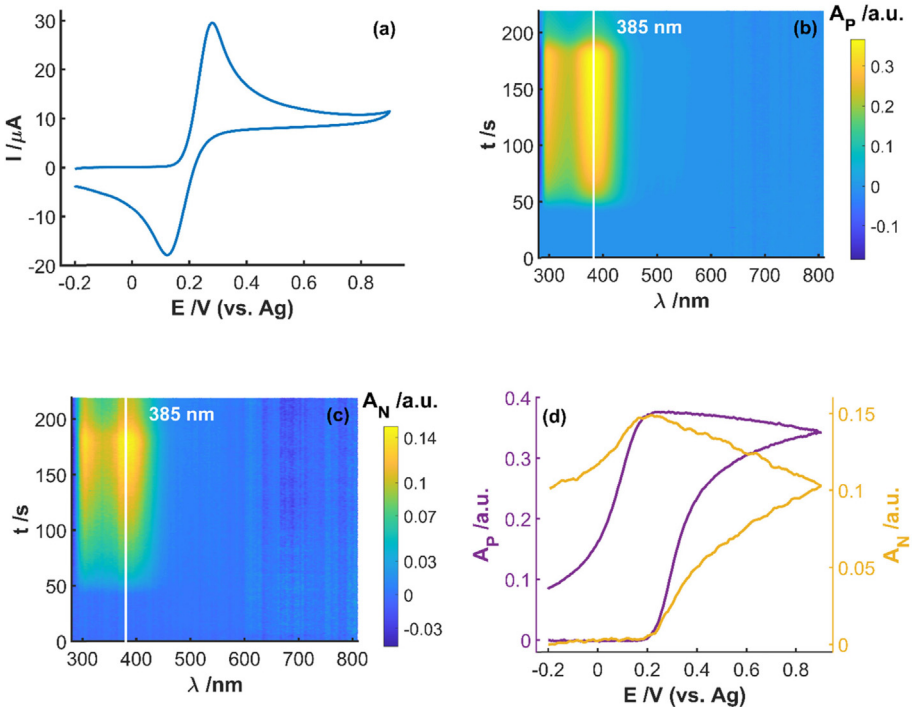

Fig. 2. BSEC experiment of $2{\cdot}10^{-3}$ M EP in 0.1 M $HClO_4$ between -0.20 V and $+0.90$ V at 0.01 V s^{-1}. (a) CV. Contour plot of the optical responses in (b) parallel and (c) normal configurations. (d) CVAs at 385 nm for the two optical configurations.

higher than that obtained in normal arrangement (0.37 a.u. vs. 0.15 a.u.), due to the longer optical path length (2 mm) in parallel configuration vs. the thickness of the diffusion layer in normal arrangement.

An acidic pH has been selected to study EP because at a higher pH the product generated during the oxidation process can polymerize, yielding an insoluble product deposited on the electrode surface [37,38]. In that case, BSEC is a very useful analytical technique because the adsorbed products are easily detected in normal direction, providing different spectra in the two optical configurations, normal and parallel [5,39]. Acidic medium allows us to work using the same electrode for all the experiments.

BSEC experiments can be useful to extract valuable information about the process taking place at the electrode surface, including the diffusion coefficients or the thickness of the diffusion layer. For this purpose, suitable models have been described in literature [6,40] which consider a precise definition of the position of the light beam interrogating the diffusion layer.

In a very simple approach, a very rough estimation of the thickness of the diffusion layer can be obtained from the ratio of the optical signal in normal and parallel configuration, knowing the distance between the two optical fibers in parallel arrangement. The ratio between the absorbance in the two configurations is proportional to the ratio between the optical pathways, and therefore, the approximate diffusion layer thickness can be calculated from Equation (1).

$$w(E) = \frac{A_N(E)d}{2A_P(E)} \tag{1}$$

where $A_N(E)$ is the absorbance in normal configuration at a specific wavelength and potential, $A_P(E)$ is the absorbance in parallel configuration at the same wavelength and potential, d is the optical pathway in parallel direction (distance between the two optical fibers) and $w(E)$ is the thickness of the diffusion layer at a specific potential, which is sampled twice in a near-normal reflection experiment. Figure S2 shows the evolution of the thickness of the diffusion layer with potential. For example, in the vertex potential, $+0.90$ V, at 385 nm a thickness of 308 μm is calculated, reaching a value of 370 μm at $+0.40$ V in the backward scan, and finally a value of 390 μm at $+0.20$ V in the backward scan. In spite of being an approximation, these values are in good agreement with the expected value which can be calculated from the approximation $w = \sqrt{\pi Dt}$.

3.2. BSEC of mixtures of EP and AA using cyclic voltammetry

After this initial spectroelectrochemical study of EP oxidation, BSEC experiments selecting cyclic voltammetry as electrochemical technique were carried out to compare the behaviors of EP, AA and a mixture of both compounds, all prepared in acidic medium (0.1 M $HClO_4$). In Fig. 3 are plotted the CVs and the corresponding CVAs at the characteristic wavelength of EPQ, 385 nm.

The CVs in Fig. 3a show the electrochemical oxidation mechanism of EP (explained in Section 3.1) and AA. The oxidation mechanism of AA is characterized by the transfer of two electrons and two protons in which dehydroascorbic acid (DHA) is electrogenerated, followed by an irreversible chemical reaction, hydrolysis of DHA, yielding 2,3-diketogulonic acid, electrochemically inactive [41]. This mechanism can be observed in the AA CV (green line, Fig. 3a), which only presents the anodic peak at +0.15 V. It should be highlighted that the oxidation of AA starts at 0 V, before the oxidation of EP, that begins at +0.15 V.

The CV corresponding to the mixture of EP and AA shows two overlapped anodic peaks, the first one related to the oxidation of AA and the second one to the oxidation of EP (orange line, Fig. 3a). Comparing the CVs of EP and the mixture of EP and AA, and considering that both solutions have the same concentration of EP, several differences can be observed. On the one hand, the anodic peak of EP is 20 % more intense in the mixture of compounds than in the solution containing only EP. On the other hand, the anodic peak potential is slightly higher in the mixed solution than in the EP solution. It can be concluded that AA interferes with the electrochemical detection of EP.

To compare the spectroscopic responses, the CVAs at 385 nm of EP, AA, and EP + AA in normal and parallel configurations are plotted in Fig. 3b. This wavelength was selected because it is related to the oxidation of EP to EPQ. For this reason, no change in absorbance values is observed in the CVAs recorded during the oxidation of the ascorbic acid solution (green lines, Fig. 3b). However, several differences can be observed between both arrangements in the signals related to EP and EP + AA solutions. In both cases, the absorbance achieved in normal configuration is lower than in parallel arrangement, which is due to the shorter optical pathway, as was explained in Section 3.1 for EP signals. Both, in normal and parallel configuration, it is observed that the oxidation of EP starts at +0.20 V. From this potential onwards, until the vertex potential, the absorbance increases due to the oxidation of EP to EPQ in a diffusion-controlled process. In the reduction scan, the absorbance decreases from +0.19 V due to the consumption of EPQ.

The absorbance value reached in the CVAs in both configurations due to the oxidation of EP in presence of AA is always lower than the absorbance value achieved in absence of this vitamin. This is due to the antioxidant effect of AA. When the potential applied is high enough, electrochemical oxidation of EP to EPQ occurs, which is then chemically reduced to EP by AA. This antioxidant effect is also responsible for the delay in detecting the increase in absorbance related to the generation of EPQ, which is noticeable from about +0.25 V. However, there are remarkable differences between normal and parallel configuration. Calculating the relative variation of absorbance at 385 nm in both configurations in the presence and absence of AA, according to Equation (2), in normal configuration absorbance in EP + AA solution is around a 35 % lower than in EP solution (blue line in Fig. 3c) from +0.35 V and +0.90 V in the anodic scan. However, in parallel configuration this difference decreases along the anodic scan from a 35 % at +0.35 V to a 1 % at +0.90 V (pink line in Fig. 3c).

$$\%\Delta A^{X}_{relative\ at\ 385\ nm} = \frac{A^{X,385\ nm}_{EP} - A^{X,385\ nm}_{EP+AA}}{A^{X,385\ nm}_{EP}} \times 100 \quad (2)$$

where absorbance values at 385 nm ($A^{385\ nm}$) correspond to the anodic scan between +0.20 V (where the oxidation of EP starts) and +0.90 V

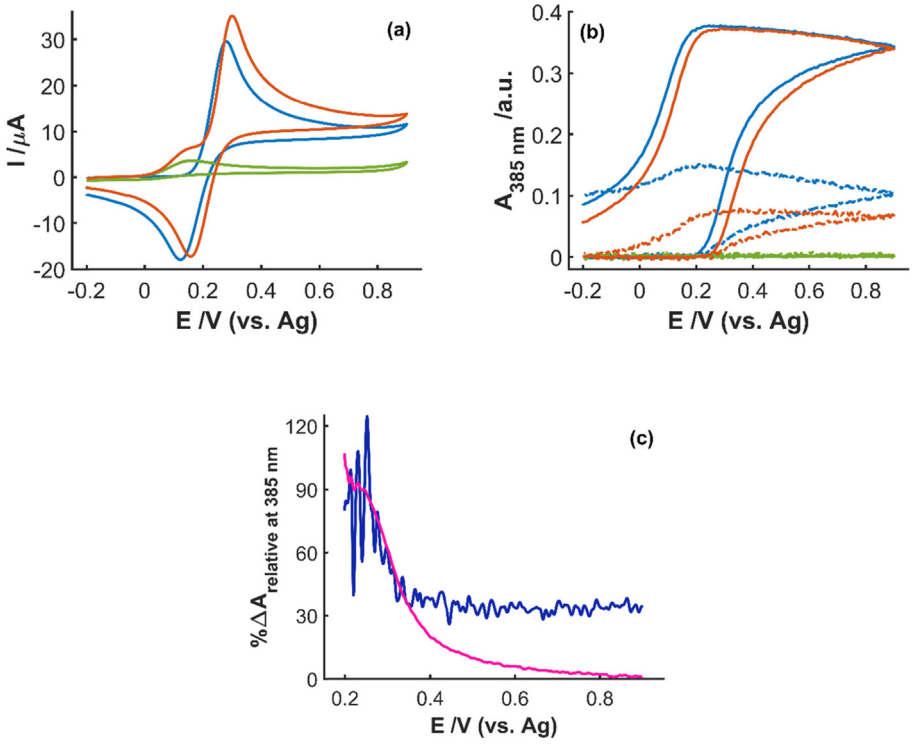

Fig. 3. Comparison between (a) CVs and (b) the corresponding CVAs at 385 nm for the BSEC experiments of $2{\cdot}10^{-3}$ M EP (blue lines), $3{\cdot}10^{-4}$ M AA (green lines), and a solution mixture of $2{\cdot}10^{-3}$ M EP and $5{\cdot}10^{-4}$ M AA (orange lines), all in 0.1 M $HClO_4$, between −0.20 V and +0.90 V at 0.01 V s^{-1}. The absorbance in normal configuration is denoted by dotted lines and the absorbance in parallel configuration by solid lines. (c) Relative variation of absorbance in normal (blue line) and parallel configuration (pink line) between the solution with EP and the one containing EP and AA in the forward scan.

(where the anodic scan ends), and *X* denotes normal or parallel configuration.

The explanation for these differences in the optical signal is related to the different regions of the solution sampled with each arrangement. In parallel configuration, approximately, only the first 120 μm of the solution adjacent to the working electrode are sampled, considering the cladding of the optical fibers. At the end of the anodic scan in this arrangement practically all the AA is oxidized, and the antioxidant effect disappears along the experiment. Consequently, the more AA is oxidized, the more EPQ is present in the diffusion layer. Conversely, in normal configuration, both the diffusion layer and the bulk solution are sampled. In the solution near the electrode the AA is oxidized to DHA along the anodic scan and its antioxidant action is less noticeable. But in the bulk solution AA still exists, which reacts with the electrogenerated EPQ that diffuses beyond 120 μm of the solution sampled by the optical fibers in parallel configuration, regenerating EP again. This causes that in normal configuration, the absorbance measured in the presence of AA is 35 % lower than that recorded in the absence of this antioxidant along the whole anodic scan.

Summarizing, as it is demonstrated, EPQ, which is the compound followed at 385 nm, only exists in the diffusion layer, corresponding to the first 120 μm of the solution adjacent to the working electrode where the amount of AA is negligible due to its electrochemical oxidation along the anodic scan and the chemical reaction of AA with EPQ. Consequently, as normal configuration provides information not only about the solution interrogated by the optical fibers, close to the electrode, but also about the bulk solution, where the presence of AA is practically constant, the differences between the absorbance values are remarkable and quite constant. In contrast, parallel configuration provides optical information only about the solution adjacent to the electrode surface, the first 120 μm, where the amount of AA greatly diminishes along the anodic scan. So, the EPQ can be successfully detected at the end of the oxidation scan in parallel configuration.

Finally, these results allow us to compare the differences between the normal and parallel configuration in a system with the presence of an antioxidant compound, understanding what signal can be used, in this case, to carry out the quantification of EP in the presence of a highly interfering species, and which ones cannot be used. In this way, as demonstrated below, the optical response in parallel configuration improves considerably the results of the EP detection using electrochemistry and the spectral response in normal arrangement, which is the most important fact to consider for carrying out the quantitative analysis.

3.3. Determination of EP in presence of AA using BSEC chronoamperometric detection

To quantify EP in presence of AA, chronoamperometric detection is selected due to its higher efficiency in the oxidation process by applying a sufficiently anodic fixed potential for a fixed time, which also shortens the length of the experiments. Since it is observed in Fig. 3a, EP is completely oxidized at +0.90 V and the process is diffusion-controlled.

BSEC chronoamperometry experiments were performed applying a potential of +0.90 V during 125 s. Fig. 4 shows chronoabsorptograms (CAbs) at 385 nm of EP, AA, and EP + AA, in normal and parallel configuration. When the potential of +0.90 V is applied, the absorbance increases because of the oxidation of EP generating EPQ (blue lines, Fig. 4). As it has been explained above, the absorbance achieved in normal configuration (dotted lines, Fig. 4) is always lower than in parallel configuration (solid lines, Fig. 4), because of the shorter optical pathway. Around 125 s, the absorbance in parallel configuration reaches a constant and maximum value, because almost all the EP in the 100 μm sampled by the light beam is transformed in EPQ. As can be inferred, the interpretation of Fig. 3 considering the different information obtained with normal and the parallel arrangements are also valid to chronoamperometric experiments depicted in Fig. 4. As shown in the CVAs in Fig. 3b, the CAbs in normal configuration for EP + AA solution is around a 35 % lower than for EP solution because of the antioxidant effect of AA (orange lines, Fig. 4). However, the antioxidant activity of AA in parallel configuration decreases significantly along the chronoamperometric experiment, reaching at 125 s almost the same absorbance value. In a similar way to CVs experiments, absorbance does not change during the whole experiment for solutions that only includes AA (green lines, Fig. 4).

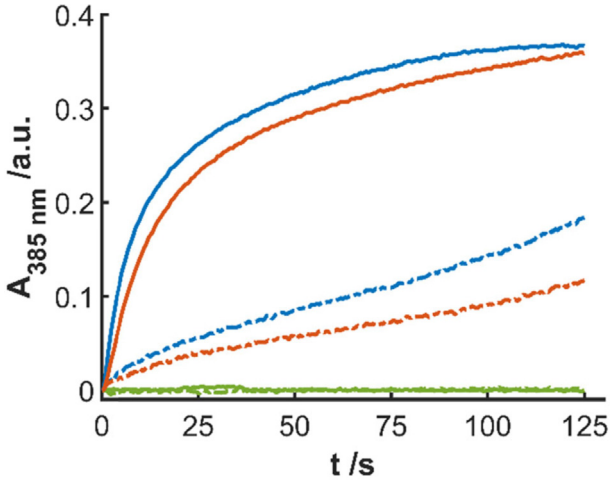

Fig. 4. Comparison between the corresponding CAbs at 385 nm for the BSEC experiments of $2{\cdot}10^{-3}$ M EP (blue lines), $3{\cdot}10^{-4}$ M AA (green lines), and a solution mixture of $2{\cdot}10^{-3}$ M EP and AA $5{\cdot}10^{-4}$ M (orange lines), all in $HClO_4$ 0.1 M, applying +0.90 V during 125 s. The absorbance in normal configuration is denoted by dotted lines and the absorbance in parallel configuration by solid lines.

From the absorbance values in normal and parallel configuration and considering Equation (1), the thickness of the diffusion layer is approximately 500 μm. Therefore, from the approximation $w = \sqrt{\pi Dt}$, an approximate diffusion coefficient of $6.37{\cdot}10^{-6}$ cm^2 s^{-1} is estimated. Assuming a similar diffusion coefficient for AA, at 125 s, few AA is located close to the optical fibers and its interference in the oxidation of EP should be really low in parallel configuration, where only the 120 μm closest to the electrode surface are interrogated.

A set of 12 chronoamperometric BSEC experiments applying +0.90 V during 125 s were performed to construct a BSEC calibration model, with the aim of demonstrating that EP can be determined not only in the absence but also in the presence of different concentrations of AA when parallel arrangement is used. Hence, different calibration

Table 1
Set of samples prepared with different concentrations of EP and AA for BSEC calibration.

Sample	C_{EP} (M)	C_{AA} (M)
01	0	0
02	$2{\cdot}10^{-3}$	0
03	0	$3{\cdot}10^{-4}$
04	$1{\cdot}10^{-3}$	$4{\cdot}10^{-4}$
05	$3{\cdot}10^{-3}$	$4{\cdot}10^{-4}$
06	$5{\cdot}10^{-4}$	$3{\cdot}10^{-4}$
07	$2{\cdot}10^{-4}$	$5{\cdot}10^{-4}$
08	$1{\cdot}10^{-4}$	$1{\cdot}10^{-4}$
09	$2{\cdot}10^{-3}$	$5{\cdot}10^{-4}$
10	$5{\cdot}10^{-3}$	$3{\cdot}10^{-4}$
11	$4{\cdot}10^{-3}$	$5{\cdot}10^{-4}$
12	0	0

samples were prepared with concentrations of EP between 0 and $5{\cdot}10^{-3}$ M in 0.1 M $HClO_4$ and with different concentrations of AA, between 0 and $5{\cdot}10^{-4}$ M (Table 1).

Each experiment provides three different signals: the chronoamperogram and two spectroscopic ones (the CAbs in normal and in parallel configuration), being able to obtain three calibration curves (Fig. 5). It should be indicated that current intensity and absorbance values in normal and parallel configuration have been obtained at 125 s after starting the experiment, that, according to Fig. 4, is the best time to quantify EP in presence of AA, particularly for the parallel configuration. The figures of merit obtained with each calibration model are tabulated in Table 2.

In the calibration curve obtained with the electrochemical data (Fig. 5a), there are some aspects that must be remarked considering that current intensity includes the oxidation of both compounds, EP and AA. There is a great difference between the two calibration points with the same concentration of $2{\cdot}10^{-3}$ M EP. The point which is above the calibration curve has $5{\cdot}10^{-4}$ M AA (sample 09), while the other point does not have AA (sample 02). Therefore, the electrochemical calibration curve is very sensitive to the presence of the interfering compound because the electrochemical signal is due to the oxidation not only of EP but also of AA. In addition, it should be highlighted that the calibration curve remarkably fails at the lowest concentrations of EP (see that the blank solution of EP in presence of AA, sample 03, gives a current intensity value very different to the expected value of zero, samples 01 and 12). Therefore, the experimental intercept is very different to the expected one if no interferent affects the quantification. Consequently, electrochemical data it is not suitable for the quantification of EP in presence of AA, even though the R^2 is close to 1.

Fig. 4b and 4d show the calibration curves obtained with the spectroscopic data, registered in normal and parallel configuration, respectively, where the absorbance at 385 nm and +0.90 V is represented versus EP concentration. It should be highlighted that also in normal configuration there is a great difference between the values with a concentration of EP of $2{\cdot}10^{-3}$ M. In this case, the point above the calibration curve has no AA (sample 02), while the point below the calibration curve has $5{\cdot}10^{-4}$ M AA (sample 09). As in the electrochemical calibration curve, the absorbance in normal arrangement is very sensitive to the presence of this interfering compound. Although this calibration curve is not adequate to predict the concentration of EP in presence of AA, there is an important advantage with respect to the electrochemical one. The intercept is very similar to the expected value of zero, because the AA does not absorb at 385 nm.

As expected from the previous sections, the figures of merit obtained when the solution is sampled in a parallel configuration are clearly better. The slope is significantly higher because of the higher optical pathlength improving the sensitivity, the intercept is very close to zero noting that AA does not absorb at this wavelength and does not interfere in the absorbance values measured, the R^2 is almost 1 and the S_{yx} is really low stating that the regression predictions fit perfectly the data. Therefore, in parallel configuration, since at 125 s there is practically no interfering effect of AA, quantification of EP in presence of AA in this concentration range can be suitably performed under these conditions (Fig. 4c and 4d).

Aiming to compare the capability of prediction of these calibration models, Table 3 shows the predicted concentrations of different measured samples of EP and AA and their relative errors. As can be observed, although none of the R^2 values are excessively far from 1 and S_{yx} values are rather low, the values obtained using the calibration model in parallel configuration are much better than those obtained for the other calibration curves. In addition, the relative errors obtained when the parallel calibration curve is used are lower than 5 %.

Thus, with these results it has been demonstrated that, the electrochemical curve is not suitable for such determination because the current intensity is associated with the oxidation of both compounds (EP

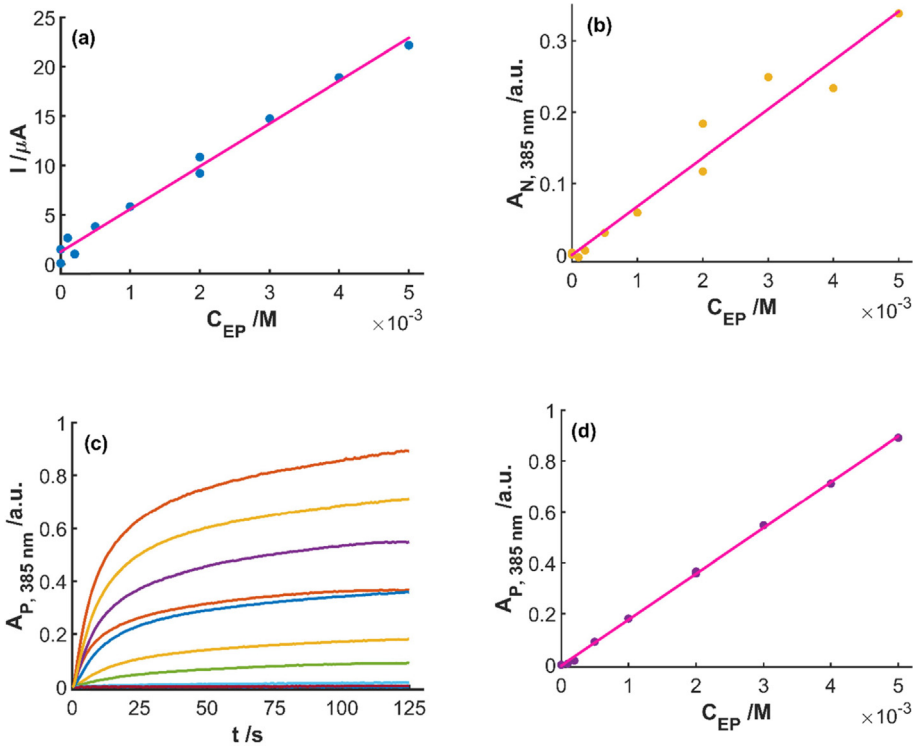

Fig. 5. Calibration curves at 125 s, after starting to apply the potential of +0.90 V, for (a) the current intensity, (b) the normal absorbance at 385 nm and (d) the parallel absorbance at 385 nm, versus EP concentration. Twelve samples with different concentrations of EP and AA were measured. (c) CAbs in parallel configuration for the 12 samples measured.

Table 2
Figures of merit for the linear regression models obtained from current intensity and absorbance values at 385 nm, +0.90 V and 125 s, in normal and parallel configuration.

Calibration model	Slope (M^{-1})	Intercept	R^2	S_{yx}
$I_{125\ s}$ vs. C_{EP}	$4.3{\cdot}10^{3}$	1.23 μA	0.9897	$8.1.10^{-1}$
$A_{N,385\ nm}$ vs. C_{EP}	$6.8{\cdot}10^{1}$	$3.0{\cdot}10^{-4}$ a.u.	0.9568	$2.7.10^{-2}$
$A_{P,385\ nm}$ vs. C_{EP}	$1.8{\cdot}10^{2}$	$-4.5{\cdot}10^{-3}$ a.u.	0.9993	$8.7.10^{-3}$

R^2: coefficient of determination; S_{yx}: standard deviation of residuals.

Table 3
Predicted concentrations with their relative errors for five different samples obtained using the calibration models in Fig. 5 and Table 2.

Calibration model	C_{EP}, REAL (M)	C_{EP}, Predicted (M)	C_{AA}, REAL (M)	% ε_r
$I_{125\ s}$ vs. C_{EP}	$5{\cdot}10^{-4}$	$5.91{\cdot}10^{-4}$	$3{\cdot}10^{-4}$	18
	$1{\cdot}10^{-3}$	$1.06{\cdot}10^{-3}$	$4{\cdot}10^{-4}$	6
	$2{\cdot}10^{-3}$	$2.21{\cdot}10^{-3}$	0	11
	$2{\cdot}10^{-3}$	$1.83{\cdot}10^{-3}$	$5{\cdot}10^{-4}$	−8
	$4{\cdot}10^{-3}$	$4.07{\cdot}10^{-3}$	$5{\cdot}10^{-4}$	2
$A_{N,385\ nm}$ vs. C_{EP}	$5{\cdot}10^{-4}$	$4.57{\cdot}10^{-4}$	$3{\cdot}10^{-4}$	−9
	$1{\cdot}10^{-3}$	$8.73{\cdot}10^{-4}$	$4{\cdot}10^{-4}$	−13
	$2{\cdot}10^{-3}$	$2.69{\cdot}10^{-3}$	0	34
	$2{\cdot}10^{-3}$	$1.71{\cdot}10^{-3}$	$5{\cdot}10^{-4}$	−14
	$4{\cdot}10^{-3}$	$3.43{\cdot}10^{-3}$	$5{\cdot}10^{-4}$	−14
$A_{P,385\ nm}$ vs. C_{EP}	$5{\cdot}10^{-4}$	$5.22{\cdot}10^{-4}$	$3{\cdot}10^{-4}$	4
	$1{\cdot}10^{-3}$	$1.03{\cdot}10^{-3}$	$4{\cdot}10^{-4}$	3
	$2{\cdot}10^{-3}$	$2.05{\cdot}10^{-3}$	0	3
	$2{\cdot}10^{-3}$	$2.01{\cdot}10^{-3}$	$5{\cdot}10^{-4}$	0.4
	$4{\cdot}10^{-3}$	$3.97{\cdot}10^{-3}$	$5{\cdot}10^{-4}$	0.8

ε_r: Relative error.

and AA). Similarly, spectroscopic in normal arrangement is not either adequate to such determination because it samples both the diffusion layer and the bulk solution. Only the spectral information in parallel configuration provides a valid calibration curve for the determination of the concentration of the analyte of interest (EP) present in a problem sample in presence of an antioxidant compound such as AA. The information provided in parallel arrangement is related to the first 120 μm adjacent to the electrode surface, where the presence of AA is practically negligible at a time greater than 125 s, thus removing the antioxidant effect at the AA concentrations studied in this work.

The results of this work demonstrate the capabilities of BSEC for analysis of EP in presence of AA, showing the negative influence of this interfering compound in the electrochemical signal and the optical signal in normal configuration, being the parallel configuration a good option to quantify EP in presence of AA. The method is robust for concentrations of AA lower than $5{\cdot}10^{-4}$ M. If AA concentrations higher than $5{\cdot}10^{-4}$ M need to be analyzed, a strategy based on a thin-layer cell can be used. For example, for $5{\cdot}10^{3}$ M EP in presence of $5{\cdot}10^{-3}$ M of AA, a difference of the signal in presence and in absence of AA lower than a 3 % is observed at 125 s in parallel direction in an experiment in a thin-layer cell (Figure S3). Moreover, the methodology presented in this work could be used to resolve more complex samples, including for example similar analytes (dopamine, L-DOPA or interfering compounds), but multivariate analysis would be needed to deconvolve the optical signals.

4. Conclusions

This work shows, for the very first time, quantitative analysis using BSEC, which is a powerful tool that permits to assess which is the best arrangement to perform quantitative measurements of an analyte in presence of a direct interfering and antioxidant compound quickly and easily. With this objective, the determination of EP in presence of AA in acidic media was selected.

It has been demonstrated that the electrochemical signal includes information of the oxidation process that occurs on the electrode surface, the oxidation of EP to EPQ and the oxidation of AA to DHA. On the other side, measurements of absorbance in normal configuration, where both the diffusion layer and the bulk solution are sampled, include information related to the distance-integrated concentration of reactants and products across the diffusion layer as a result of the oxidation reaction at the electrode surface. In the problem tackled in this work, the presence of AA significantly affects the detection of EP, being neither possible to quantify it correctly.

Conversely, absorbance in parallel arrangement allows the determination of EP despite the presence of AA. For this purpose, a sufficiently high potential has been chosen to effectively oxidize both, AA and EP, in order to practically eliminate the antioxidant effect of AA. In this case, sampling approximately the 120 μm of the solution adjacent to the working electrode in parallel configuration, where only the diffusion layer is observed, the amount of AA at long enough times can be negligible due to its electrochemical oxidation and the chemical reaction with EPQ. Actually, the process is more complicated because the formal potential of the two redox couples (AA/DHA and EP/EPQ) are very close, as is observed in Fig. 3. Therefore, the methodology shown in this work is effective for AA concentrations lower than $5{\cdot}10^{-4}$ M, since the diffusion of AA from the bulk solution in more concentrated solutions can interfere in the optical response. For higher concentrations, working in a thin-layer setup would be mandatory in order to avoid the diffusion of the interfering compound from the bulk solution. In summary, while the electrochemical and normal absorbance predicted values are very sensitive to the presence of the antioxidant species in the sample, the parallel absorbance provides excellent results to quantify EP in presence of AA, which should be extrapolated to equivalent systems. Always, spectroelectrochemistry users must take care to select appropriate experimental conditions to electrochemically remove the interfering compounds.

This paper increases the advantages of spectroelectrochemistry in terms of selectivity, as well as demonstrates the need to select properly the optical mode to carry out the analysis of the compounds, being very important to know which configuration is more convenient to select in each case. This strategy lays the groundwork for spectroelec-

troanalysis for cases in which antioxidant compounds are present in the solution.

Data availability

Data will be available at the Universidad de Burgos data repository

Declaration of Competing Interest

The authors declare that they have no known competing financial interests or personal relationships that could have appeared to influence the work reported in this paper.

Acknowledgments

Authors acknowledge the financial support given by Ministerio de Ciencia e Innovación and Agencia Estatal de Investigación (MCIN/AEI/ 10.13039/501100011033, PID2020-113154RB-C21) and Ministerio de Ciencia, Innovación y Universidades (Grant RED2018-102412-T). Fabiola Olmo is grateful for the contract funded by Junta de Castilla y León, the European Social Fund, and the Youth Employment Initiative.

Appendix A. Supplementary data

Supplementary data to this article can be found online at https://doi.org/10.1016/j.jelechem.2023.117333.

References

[1] J. Garoz-Ruiz, J.V. Perales-Rondon, A. Heras, A. Colina, Spectroelectrochemical Sensing: Current Trends and Challenges, Electroanalysis. 31 (2019) 1254–1278, https://doi.org/10.1002/elan.201900075.
[2] J.J.A. Lozeman, P. Führer, W. Olthuis, M. Odijk, Spectroelectrochemistry, the future of visualizing electrode processes by hyphenating electrochemistry with spectroscopic techniques, Analyst. 145 (2020) 2482–2509, https://doi.org/10.1039/C9AN02105A.
[3] Y. Zhai, Z. Zhu, S. Zhou, C. Zhu, S. Dong, Recent advances in spectroelectrochemistry, Nanoscale. 10 (2018) 3089–3111, https://doi.org/10.1039/C7NR07803J.
[4] J. Garoz-Ruiz, A. Heras, S. Palmero, A. Colina, Development of a Novel Bidimensional Spectroelectrochemistry Cell Using Transfer Single-Walled Carbon Nanotubes Films as Optically Transparent Electrodes, Anal. Chem. 87 (2015) 6233–6239, https://doi.org/10.1021/acs.analchem.5b00923.
[5] J. López-Palacios, A. Colina, A. Heras, V. Ruiz, L. Fuente, Bidimensional Spectroelectrochemistry, Anal. Chem. 73 (2001) 2883–2889, https://doi.org/10.1021/ac0014459.
[6] L. Romay, J. González, Á. Molina, E. Laborda, Investigating Comproportionation in Multielectron Transfers via UV–Visible Spectroelectrochemistry: The Electroreduction of Anthraquinone-2-sulfonate in Aqueous Media, Anal. Chem. 94 (2022) 12152–12158, https://doi.org/10.1021/acs.analchem.2c02523.
[7] Y.P. Gui, T. Kuwana, Long Optical Path Length Thin-Layer Spectroelectrochemistry: Hydrogenation of Adsorbed Aromatics by Coadsorbed Hydrogen Atoms at Platinum, Langmuir. 2 (1986) 471–476, https://doi.org/10.1021/la00070a017.
[8] F. Kusu, T. Kuwana, Long Optical Path Length Thin-Layer Spectrochemistry Potential Dependence and Quantitation of 1 H -Purine-6-amine Adsorbed on Gold, Chem. Lett. 17 (1988) 531–534, https://doi.org/10.1246/cl.1988.531.
[9] J. Garoz-Ruiz, A. Heras, A. Colina, Simultaneous study of different regions of an electrode surface with a novel spectroelectrochemistry platform, Electrochem. Commun. 90 (2018) 73–77, https://doi.org/10.1016/j.elecom.2018.04.006.
[10] N. González-Diéguez, A. Colina, J. López-Palacios, A. Heras, Spectroelectrochemistry at Screen-Printed Electrodes: Determination of Dopamine, Anal. Chem. 84 (2012) 9146–9153, https://doi.org/10.1021/ac3018444.
[11] E. Laborda, J. García-Martínez, A. Molina, Spectroelectrochemistry for the study of reversible electrode reactions with complex stoichiometries, Electrochem. Commun. 123 (2021), https://doi.org/10.1016/j.elecom.2020.106915 106915.
[12] J. Garoz-Ruiz, C. Guillen-Posteguillo, A. Heras, A. Colina, Simplifying the assessment of parameters of electron-transfer reactions by using easy-to-use thin-layer spectroelectrochemistry devices, Electrochem. Commun. 86 (2018) 12–16, https://doi.org/10.1016/j.elecom.2017.11.001.
[13] F. Olmo, J. Garoz-Ruiz, A. Colina, A. Heras, Derivative UV/Vis spectroelectrochemistry in a thin-layer regime: deconvolution and simultaneous quantification of ascorbic acid, dopamine and uric acid, Anal. Bioanal. Chem. 412 (2020) 6329–6339, https://doi.org/10.1007/s00216-020-02564-1.
[14] W. Wang, H.M. Grace, P.A. Flowers, Simple microfluidic device for spectroelectrochemistry, Microchem. J. 181 (2022), https://doi.org/10.1016/j.microc.2022.107718 107718.
[15] L.G. Oliveira, S.G. Lemos, W.D. Fragoso, Simultaneous determination of benzenediol isomers in tap water by second-order calibration and voltabsorptometry, Electrochim. Acta. 354 (2020), https://doi.org/10.1016/j.electacta.2020.136591 136591.
[16] A. Ghoorchian, A. Afkhami, T. Madrakian, R. Rameshan, C. Rameshan, A. Hajian, Absorbance-based Spectroelectrochemical Sensor for Determination of Ampyra Based on Electrochemical Preconcentration, Sensors Actuators, B Chem. 324 (2020), https://doi.org/10.1016/j.snb.2020.128723 128723.
[17] H. Ali, N. Verma, A Hybrid UV-Vis Spectroelectrochemical Approach for Measuring Folic Acid using a Novel Ni-CNF/ITO Electrode, Electrochim. Acta. 428 (2022), https://doi.org/10.1016/j.electacta.2022.140920 140920.
[18] G. Sirin Ustabasi, J. Bastos-Arrieta, C. Pérez-Ràfols, N. Serrano, J.M. Díaz-Cruz, Considerations on the use of spectroelectrochemistry in reflection mode for quantitative analysis: Study of the Fe(III)/Fe(II) – orthophenanthroline system, Microchem. J. 181 (2022), https://doi.org/10.1016/j.microc.2022.107678 107678.
[19] J. Garoz-Ruiz, C. Guillen-Posteguillo, A. Colina, A. Heras, Application of spectroelectroanalysis for the quantitative determination of mixtures of compounds with highly overlapping signals, Talanta. 195 (2019) 815–821, https://doi.org/10.1016/j.talanta.2018.12.002.
[20] J. López-Palacios, A. Heras, Á. Colina, V. Ruiz, Bidimensional spectroelectrochemical study on electrogeneration of soluble Prussian Blue from hexacyanoferrate(II) solutions, Electrochim. Acta. 49 (2004) 1027–1033, https://doi.org/10.1016/j.electacta.2003.10.013.
[21] V. Ruiz, Á. Colina, A. Heras, J. López-Palacios, R. Seeber, Bidimensional chronoabsorptometric study of electropolymerisation of 4,4′-bis(2-methylbutylthio)-2,2′-bithiophene, Electrochem. Commun. 4 (2002) 451–456, https://doi.org/10.1016/S1388-2481(02)00325-9.
[22] T. Flatmark, Catecholamine biosynthesis and physiological regulation in neuroendocrine cells, Acta Physiol. Scand. 168 (2000) 1–17, https://doi.org/10.1046/j.1365-201X.2000.00596.x.
[23] J. Harley-Mason, The chemistry of adrenochrome and its derivatives, J. Chem. Soc. (1950) 1276–1282, https://doi.org/10.1039/jr9500001276.
[24] M.D. Hawley, S.V. Tatawawadi, S. Piekarski, R.N. Adams, Electrochemical studies of the oxidation pathways of catecholamines, J. Am. Chem. Soc. 89 (2) (1967) 447–450.
[25] H. Cui, L. Wu, J. Chen, X. Lin, Multi-mode in situ spectroelectrochemical studies of redox pathways of adrenaline, J. Electroanal. Chem. 504 (2001) 195–200, https://doi.org/10.1016/S0022-0728(01)00444-2.
[26] P. Hernández, I. Sánchez, F. Patón, L. Hernández, Cyclic voltammetry determination of epinephrine with a carbon fiber ultramicroelectrode, Talanta. 46 (5) (1998) 985–991.
[27] K.-H. Xue, J.-M. Liu, R.-B. Wei, S.-P. Chen, Electrochemical behavior of adrenaline at the carbon atom wire modified electrode, Chem. Phys. 327 (2006) 319–326, https://doi.org/10.1016/j.chemphys.2006.05.004.
[28] S.S. Shankar, R.M. Shereema, R.B. Rakhi, Electrochemical Determination of Adrenaline Using MXene/Graphite Composite Paste Electrodes, ACS Appl. Mater. Interfaces. 10 (2018) 43343–43351, https://doi.org/10.1021/acsami.8b11741.
[29] S.H. Kim, I.-H. Yeo, Spectroelectrochemical Studies on the Oxidation Pathway of Epinephrine, Anal. Sci. 13 (1997) 321–324, https://doi.org/10.2116/analsci.13.Supplement_321.
[30] S.H. Kim, J.W. Lee, I.-H. Yeo, Spectroelectrochemical and electrochemical behavior of epinephrine at a gold electrode, Electrochim. Acta. 45 (2000) 2889–2895, https://doi.org/10.1016/S0013-4686(00)00364-9.
[31] A. Salimi, H. MamKhezri, R. Hallaj, Simultaneous determination of ascorbic acid, uric acid and neurotransmitters with a carbon ceramic electrode prepared by sol–gel technique, Talanta. 70 (2006) 823–832, https://doi.org/10.1016/j.talanta.2006.02.015.
[32] N. Nasirizadeh, Z. Shekari, H.R. Zare, M. Reza Shishehbore, A.R. Fakhari, H. Ahmar, Electrosynthesis of an imidazole derivative and its application as a bifunctional electrocatalyst for simultaneous determination of ascorbic acid, adrenaline, acetaminophen, and tryptophan at a multi-wall carbon nanotubes modified electrode surface, Biosens. Bioelectron. 41 (2013) 608–614, https://doi.org/10.1016/j.bios.2012.09.028.
[33] E. Wierzbicka, M. Szultka-Młyńska, B. Buszewski, G.D. Sulka, Epinephrine sensing at nanostructured Au electrode and determination its oxidative metabolism, Sensors Actuators B Chem. 237 (2016) 206–215, https://doi.org/10.1016/j.snb.2016.06.073.
[34] P. Pradhan, R.J. Mascarenhas, T. Thomas, I.N.N. Namboothiri, O.J. D'Souza, Z. Mekhalif, Electropolymerization of bromothymol blue on carbon paste electrode bulk modified with oxidized multiwall carbon nanotubes and its application in amperometric sensing of epinephrine in pharmaceutical and biological samples, J. Electroanal. Chem. 732 (2014) 30–37, https://doi.org/10.1016/j.jelechem.2014.08.023.
[35] G.P. Jin, X. Peng, Y.F. Ding, The electrochemical modification of clenbuterol for biosensors of dopamine, norepinephrine, adrenalin, ascorbic acid and uric acid at paraffin-impregnated graphite electrode, Biosens. Bioelectron. 24 (2008) 1031–1035, https://doi.org/10.1016/j.bios.2008.06.028.
[36] G.J. Yang, J.J. Xu, H.Y. Chen, The study of redox mechanism of dobutamine at different pH media by electrochemical and in situ spectroelectrochemical methods, Electrochim. Acta. 49 (2004) 3121–3127, https://doi.org/10.1016/j.electacta.2004.02.026.

[37] R. Abdel-Hamid, E.F. Newair, Adsorptive stripping voltammetric determination of gallic acid using an electrochemical sensor based on polyepinephrine/glassy carbon electrode and its determination in black tea sample, J. Electroanal. Chem. 704 (2013) 32–37, https://doi.org/10.1016/j.jelechem.2013.06.006.

[38] Z.F. Gao, T.T. Li, X.L. Xu, Y.Y. Liu, H.Q. Luo, N.B. Li, Green light-emitting polyepinephrine-based fluorescent organic dots and its application in intracellular metal ions sensing, Biosens. Bioelectron. 83 (2016) 134–141, https://doi.org/10.1016/j.bios.2016.04.041.

[39] V. Ruiz, Á. Colina, A. Heras, J. López-Palacios, R. Seeber, Bidimensional spectroelectrochemistry applied to the electrosynthesis and characterization of conducting polymers: Study of poly[4,4′-bis(butylthio)-2,2′-bithiophene], Helv. Chim. Acta. 84 (2001) 3628–3642, https://doi.org/10.1002/1522-2675(20011219)84:12<3628::AID-HLCA3628>3.0.CO;2-0.

[40] A. Colina, J. López-Palacios, A. Heras, V. Ruiz, L. Fuente, Digital simulation model for bidimensional spectroelectrochemistry, J. Electroanal. Chem. 553 (2003) 87–95, https://doi.org/10.1016/S0022-0728(03)00288-2.

[41] A.M. Pisoschi, A. Pop, A.I. Serban, C. Fafaneata, Electrochemical methods for ascorbic acid determination, Electrochim. Acta. 121 (2014) 443–460, https://doi.org/10.1016/j.electacta.2013.12.127.